RSC Advances

ROYAL SOCIETY OF CHEMISTRY

www.rsc.org/advances

RSC Advances

RSCPublishing

ARTICLE

Two Novel Ambipolar Donor-Acceptor Type Electrochromic Polymers with the Realization of RGB (Red-Green-Blue) Display in one Polymer

Hui Zhao[1], Daidi Tang[1,2], Jinsheng Zhao[2,*], Min Wang[2] and Jianmin Dou[2,*]

Cite this: DOI: 10.1039/x0xx00000x

Received 00th January 2012,
Accepted 00th January 2012

DOI: 10.1039/x0xx00000x

www.rsc.org/

Two novel electrochromic monomers, 4,7-bis(4-methoxythiophen-2-yl)-[1,2,5]thiadiazolo[3,4-c]pyridine (MOTTP) and 4,7-bis(4-butoxythiophen-2-yl)-[1,2,5]thiadiazolo[3,4-c]pyridine (BOTTP) were synthesized and electropolymerized to give corresponding polymers PMOTTP and PBOTTP, respectively. For investigated its electrochemical and electrochromic properties, the polymers were characterized by cyclic voltammetry (CV), UV–vis spectroscopy, step profiler, and scanning electron microscopy (SEM). The band gap of polymers were calculated based on the spectroelectrochemistry analysis, and were 0.950 eV and 1.088 eV for PMOTTP and PBOTTP, respectively. Electrochromic investigations showed that PMOTTP and PBOTTP performed similarly multichromic behavior; saturation green color in the neutral state, highly transmissive blue in the oxidized state, and saturation red in the reduced state (RGB). In addition, both polymers have excellent switching properties with more than 60% optical contrasts in the NIR region and about 0.5 s response time from neutral to oxide. Moreover, via electrochemical and spectral analyses both polymers were proven to be n-type dopable polymers. Hence, both polymers are promising material to complete RGB electrochromic polymers for the commercial application.

Introduction

Since the discovery of the conductivity of the dopped polyacetylene,[1] the study in the field of conducting polymers attracts more and more scientists being engaged in it. Over the past decades, conjugated polymers showed great potentials for the applications in organic electronic devices, such as photovoltaic devices,[2] light-emitting diodes (LEDs),[3] field effect transistors,[4] sensors,[5] and electrochromic devices.[6-8] Electrochromism is defined as a reversible change in color, or optical density of a substance induced by a change in voltage or electric potential.[9,10] Although the earliest electrochromic devices are mostly based on inorganic oxides, such as tungsten, iridium, nick oxides,[11] etc., the use of conjugated polymers as active layers in electrochromic devices has received enormous attention because of their high optical contrasts,[12] fast switching times,[13,14] processability,[15] and fine-tuning of the band gap by structure modification[7]. Up to date, types of electrochromic devices include smart windows,[16] rear-view mirrors[3] for cars and electrochromic displays. As a kind of important electron-rich heterocycle based polymers, polythiophene and its derivatives are the most commonly used conjugated polymer materials for electrochromic purpose because of their flexibility towards synthetic modifications.

Red, green, blue (RGB) are the three main colors for display technology since all other subtractive colors can be achieved by mixing these three.[17] Among RGB colors, neutral state green polymers with highly transmissive oxidized states are very difficult to get. This is because that to obtain a neutral green polymer, two absorption bands are necessary, one in the red region of the spectrum, and the other in the blue region, leaving an absorption trough in the green region of the spectrum. Furthermore, the two absorption bands should be controlled with the same applied potential, and disappear simultaneously upon successive oxidation to give a bleached transmissive oxidation state.[18] The band gaps of the neutral green to transmissive switching polymers are usually less than 1.2 eV, which can only be achieved by the means of a donor-acceptor approach. Donor-acceptor systems lead to a narrower band gap because of resonances that enable a stronger double bond character between the donor and acceptor units.[19] Since the report of the first neutral green polymer in 2004, a soluble bithiophene-thienopyrazine copolymer by the Wudl group,[20] which had a non-transmissive oxidation state, a few of green-to-transmissive polymers have been reported by the Reynolds group,[21] the Toppare group,[22] and the Cihaner group, etc. These studies open the way of commercialization for electrochromic display devices. However, in the context of low cost and high performance display devices, the main demand is becoming to achieve multi-colored redox achievable states from a single polymer. Up to date, the examples of neutral state green polymeric materials have still been very rare,[23-24] especially the ones with additional multicolored property are welcome.

For the construction of D-A-D type monomers, ethylenedioxythiophene (EDOT) and thiophene derivatives are usually used as the donor units. Meanwhile, 1,2,3-benzotriazole, quinoxaline,[25-27] thieno[3,4-b]pyrazine, 2,1,3-benzothiadiazole (BTD) and benzoselenadiazole(BSE)[28] are the mosty preferred acceptor type units. The [1, 2, 5]thiadiazolo[3,4-*c*]pyridine (PT) hetero cycle has been employed as an electron-deficient unit in the synthesis of the polymer photovoltaic materials and panchromatic organic sensitizers for Dye-sensitized mesoscopic

solar cells.[29,30] Compared with the BTD unit, the PT is a stronger acceptor[20] due to the presence of the additional pyridine N-atoms.

The donor-acceptor type polymer (PTBT) synthesized with benzotriazole as the acceptor unit and thiophene as the donor unit revealed all three additive colors (RGB) at different oxidation states, and also showed both n- and p-dopable characteristics.[31] The discovery of RGB displaying polymers make it possible for the construction of a single component electrochromic display device. Very limited progress concerning the synthesis of RGB displaying polymers has been made since the discovery of PTBT. By employing 3-alkoxy thiophene as the donor unit and PT as the acceptor unit, We report here the synthesis and electrochemical properties of two newly designed donor-acceptor type electrochromic polymers poly [4,7-bis(4-methoxythiophen-2-yl)-[1,2,5]thiadiazolo[3,4-c]pyridine] (PMOTTP) and poly [4,7-bis(4-butoxythiophen-2-yl)-[1,2,5]thiadiazolo[3,4-c]pyridine] (PBOTTP). Both polymers are green in their neutral states and revealed highly transmissive blue in their oxidized state, and saturation red in their reduced states. Effects of the length of the alkyl chains in the donor unit on electrochemical and spectral behavior of the resulting polymers were also discussed in detail.

Experimental

General

All chemicals except indicated otherwise were purchased from commercial sources and used without further purification except tetrahydrofuran which was distilled over Na/benzophenone prior to be used. 2,5-dibromopyridine-3,4-diamine,[32,33] 4,7-dibromo-[1,2,5]thiadiazolo[3,4-c]pyridine[32,33] and tributylstannane[34] compounds were prepared according to the literature method. ^{1}H NMR and ^{13}C NMR spectroscopy studies were carried out on a Varian AMX 400 spectrometer and the chemical shifts (δ) were given relative to tetramethylsilane as the internal standard. Electrochemical synthesis and experiments were performed in a one-compartment cell with a CHI 760 C Electrochemical Analyzer controlled by a computer, employing a platinum wire with a diameter of 0.5 mm as working electrode, a platinum ring as counter electrode, and a Ag wire (0.02 V vs. SCE.) as pseudo-reference electrode. Before and after each experiment, the silver pseudo reference was calibrated versus the ferrocene redox couple and then adjusted to match the SCE reference potential. Electrodeposition was performed from a 0.2 M solution of tetrabutylammonium hexafluorophosphate ($TBAPF_6$) at scan rate of 100 mVs^{-1} for 20 cycles. Scanning electron microscopy (SEM) measurements were taken by using a Hitachi SU-70 thermionic field emission SEM. The thickness and surface roughness of polymer films were carried on KLA-Tencor D-100 step profiler. UV-Vis-NIR spectra were recorded on a Varian Cary 5000 spectrophotometer connected to a computer. A three-electrode cell assembly was used for spectroelectrochemistry measurement where the working electrode was an indium tin oxide (ITO) glass, the counter electrode was a stainless steel wire, and an Ag wire was used as pseudo reference electrode. The polymer films for spectroelectrochemistry were prepared by potentiostatically deposition on ITO glass slides (the active area: 1.0 cm × 2.8 cm). The thickness of the polymer films grown potentiostatically on ITO was controlled by the total charge passed through the cell and was measured by step profiler. Digital photographs of the polymer films were taken by a Canon Power Shot A3000 IS digital camera. Elemental analyses are determined by a Thermo Finnigan Flash EA 1112, CHNS-O elemental analyses instrument. Mass spectrometry analysis was conducted using a Bruker maXis UHR-TOF mass spectrometer.

Synthesis procedure

2,5-dibromopyridine-3,4-diamine

The mixture of pyrido-3,4-diamine(2 g, 18.3 mmol) with an aqueous HBr (48%, 30 ml) were prepared in a 250 ml three-neck round-bottom flask with a magneton inside. After the mixture was heated to 100 ºC, bromine (2.5 ml) was added dropwise, and the solution was stirred for 5 h at 135 ºC. The mixture was cooled to room temperature, an aqueous solution of $Na_2S_2O_3$, an aqueous solution of Na_2CO_3, and distilled water were added in this order to get a yellow precipitate. Then the precipitate was separated by filtration and washed by distilled water three times. Recrystallization from the mixture solution of toluene:THF (v:v=5:1) gave white flocculence of 3,4-diamino-2,5-dibrompyridine(yield = 51%). Mp:216-218 °C. ^{1}H NMR (400MHz, DMSO, δ/ppm): 7.53 (s, 1H, pyridic-H), 5.99 (s, 2H, N-H), 5.03 (s, 2H, N-H). ^{13}CNMR (100 MHz, $CDCl_3$, δ/ppm): 139.93, 139.13, 129.54, 126.67, 106.22. MS ($C_5N_3Br_2H_5$) m/z: calcd for 266.9; found 266.8. Anal. Calcd for ($C_5N_3Br_2H_5$): C, 22.5; N, 15.7; Br, 59.9; H, 1.9. Found: C, 22.4; N, 15.7; Br, 60.0, H, 1.9.

4,7-dibromo-[1,2,5]thiadiazolo[3,4-c]pyridine

To a 100 ml there-neck round bottom flask equipped with a magnetic stirring bar, 2,5-dibromopyridine-3,4-diamine(1.1g, 3.8 mmol) and pyridine (12 mL) were added successively under nitrogen atmosphere. The $SOCl_2$ (0.7 mL) was then dropped, the resulting mixture was stirring at 0 ºC until a deep pink colored solution was obtained. This was followed by reflux at 80 ºC overnight. The reaction mixture was allowed to cool to room temperature. The reaction mixture was filtered and washed with water repeatedly, dried over anhydrous $MgSO_4$. The crude mixture was chromatographed on silica gel by eluting with hexane/ dichloromethane (4:1, v/v) to give the yellow solid. Mp: 115 °C. ^{1}H NMR (300 MHz, $CDCl_3$, δ/ppm): 8.552 (s, 1H, pyridic-H). ^{13}CNMR (100 MHz, $CDCl_3$, δ/ppm): 162.79, 160.88, 153.17, 139.18, 96.22. MS ($C_5SN_3Br_2H$) m/z: calcd for 294.9; found 294.7. Anal. Calcd for ($C_5SN_3Br_2H$): C, 20.4; S, 10.9; N, 14.2; Br, 54.2; H, 0.3. Found: C, 20.3; S, 10.8; N, 14.3; Br, 54.3; H, 0.3.

General procedure for the synthesis of MOTTP and BOTTP via Stille Coupling

4,7-dibromo-[1,2,5]thiadiazolo[3,4-c]pyridine (1.00 g, 3.4 mmol), and the excessive tributyl(3-methoxythiophen-2-yl)stannane (17 mmol) or tributyl(3-butoxythiophen-2-yl)stannane (17 mmol) using $Pd(PPh_3)_2Cl_2$ (0.238 g, 0.34 mmol) as the catalyst were dissolved in anhydrous toluene (80 mL) at room temperature. The solution was stirred under nitrogen atmosphere for 30 min. Raise the temperature immediately until the solution was refluxed. The mixture was stirred under

nitrogen atmosphere for 24 h, cooled and concentrated on the rotary evaporator. Lastly the residue was purified by column chromatography on silica gel using hexane- dichloromethane as the eluent.

4,7-bis(4-methoxythiophen-2-yl)-[1,2,5]thiadiazolo[3,4c]pyridine (MOTTP)

The crude mixture was chromatographed on silica gel by eluting with hexane: dichloromethane (1:2, v/v) to give MOTTP as red solid (0.8 g, 67%).Mp:186 °C. ^{1}H NMR (400 MHz, $CDCl_3$, δ/ppm): 8.77 (s, 1H, pyridic-H), 8.34 (d, 1H, thienyl-H), 7.77 (d, 1H, thienyl-H), 6.56 (d, 1H, thienyl-H), 6.42 (d, 1H, thienyl-H), 3.89 (d, 6H,-OCH_3). ^{13}CNMR (100 MHz, $CDCl_3$, δ/ppm):159.55, 159.17, 146.28, 140.50, 135.27, 123.34, 120.02, 103.19, 99.27, 57.56. MS ($C_{13}H_{11}N_3S_3O_2$) m/z: calcd for 337.4; found 337.5. Anal. Calcd for ($C_{13}H_{11}N_3S_3O_2$): C, 46.3; N, 12.4; O, 9.5; S, 28.5; H, 3.3. Found: C, 46.5; N, 12.4; O, 9.4; S, 28.3; H, 3.4.

4, 7-bis(4-butoxythiophen-2-yl)-[1,2,5]thiadiazolo[3,4-c]pyridine (BOTTP)

The crude mixture was chromatographed on silica gel by eluting with hexane: dichloromethane (1:3, v/v) to give BOTTP as red solid (0.76 g, 50%). Mp:149 °C. ^{1}H NMR (400 MHz, $CDCl_3$, δ/ppm): 8.78 (s, 1H, pyridic-H), 8.38 (d, 1H, thienyl-H), 7.78 (d, 1H, thienyl-H), 6.55 (d, 1H, thienyl-H), 6.41 (d, 1H, thienyl-H), 4.03 (m, 4H, -OCH_2), 1.81 (m, 4H,-CH_2), 1.33 (m, 4H,-CH_2), 0.99 (t, 6H,-CH_3). ^{13}CNMR (100 MHz, $CDCl_3$, δ/ppm): 158.47, 154.97,146.34, 139.66, 135.01, 123.89, 120.29, 103.62, 99.61, 70.22, 31.53, 19.47, 14.05. MS ($C_{13}H_{23}N_3S_3O_2$) m/z: calcd for 349.5; found 349.4. Anal. Calcd for ($C_{13}H_{23}N_3S_3O_2$): C, 44.7; N, 12.0%; O, 9.2%, S, 27.5: H, 6.6%. Found: C, 44.5; N, 12.1%; O, 9.2%, S, 27.7: H, 6.5%.

Result and discussion

Synthesis of monomers

The synthesis of MOTTP and BOTTP was carried out with slight modifications of the well-established literature procedures (Scheme 1). The first step of this route involved the bromination of pyridine-3,4-diamine in the presence of HBr/Br_2 mixture. The second step, 4,7-dibromo-[1,2,5]thiadiazolo[3,4-c]pyridine was given through oxidation with an excess amount of $SOCl_2$ in pyridine solvent. The organotin compound was synthesized follow previously literature.[35] The last step, the Stille coupling reaction was achieved in anhydrous toluene in the presence of a catalytic amount of $Pd(PPh3)_2Cl_2$. The reactions proceeded quite nicely to afford MOTTP and BOTTP with satisfactory yields.

Electrochemical polymerization

The electrochemical properties of monomers and their polymers were examined by using cyclic voltammetry. All polymers were deposited on Pt wire by cyclic voltammetry with the same scan rate (100 mVs^{-1}) in acetonitrile (ACN)/dichloromethane (DCM) (1:1, by volume) solvent mixture containing 0.2 M tetrabutylammonium hexafluorophosphate ($TBAPF_6$) as the supporting electrolyte and 0.005 M monomers. Voltammetry curves for the repeated scanning electropolymerization of MOTTP and BOTTP were shown in Fig.1. The first cycle of the CV test ascribed oxidation of monomer and the onset oxidation potentials (E_{onset}) of MOTTP and BOTTP are 1.06 and 1.07 V, respectively. During the repetitive anodic potential scan, the generation of a new quasi-reversible redox couple (E_p^{ox} = 0.77 V, E_p^{red} = 0.62 V for MOTTP and E_p^{ox} = 0.81, E_p^{red} = 0.82 V for BOTTP) and the increase in the current intensity of this quasi-reversible redox peak indicated the formation of highly electroactive polymers on the surface of working electrodes. By contrast, the oxidation potential of MOTTP was lower than that of BOTTP since the electron donating effect of BOTTP was decreased due to the steric bulky groups introduced by the butyl chains , resulting in a less efficient overlapping between the π-orbital of oxygen atom and the conjugated system. It can thus be concluded that the redox reaction is highly sensitive to the steric and electronic effects of the substituent.[35]

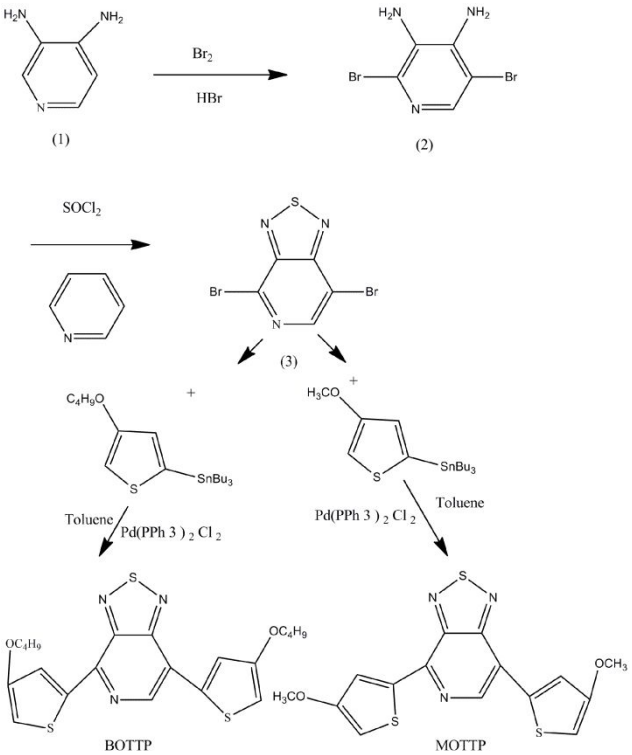

Scheme 1 Synthetic route of the monomers.

Electrochemical behaviors of polymer films (prepared on platinum wires by sweeping the potentials three cycles) were characterized by CV method at different scan rates between 25 and 300 mVs^{-1} in monomer free electrolyte solution. The CV curves of PMOTTP and PBOTTP at different scan rates between 25 and 300 mVs^{-1} in p-doping process were shown in Fig.2a and Fig.2b, respectively. It was clearly observed a couple of redox peaks with an oxidation potential of 0.79 V and a reduction potential of 0.74 V in the p-doping process for PMOTTP. A couple of redox peaks of PBOTTP were located at 0.91 and 0.80 V, respectively. The scan rate dependence of the peak currents density was illustrated in Fig. 2c. As seen in Fig. 2c, the peak currents density reveal a linear relationship as a function of scan rate for both polymers, which indicates that the electrochemical processes are not diffusion limited and are quasi-reversible even at high scan rates.[8] The CV of PMOTTP

and PBOTTP at scan rate of 100 mVs^{-1} during n-doping and p-doping process was shown in Fig.2d. It can be seen a quasi-reversible p-style doping and a quasi-reversible n-style doping. In the reduction region, a sharp redox peak (E_p^{ox} = -0.87 V, E_p^{red} = -0.78 V for PMOTTP and E_p^{ox} = -0.88, E_p^{red} = -0.79 V for PBOTTP) is observed which indicates the polymer has the n-dopable character. Furthermore, it was notable that the redox peaks of the n-doping/dedoping were much stronger than the p-doping/dedoping process. The results indicated that [1,2,5]thiadiazolo[3,4-c]pyridine (PT) was a strong electron acceptor and PMOTTP and PBOTTP were a good n-type conjugated polymers. As clearly stated in literature,[36] negatively doped waves in CV do not necessarily mean that a true n-type doping process is available. Hence, additional support must be given via spectroelectrochemistry studies.

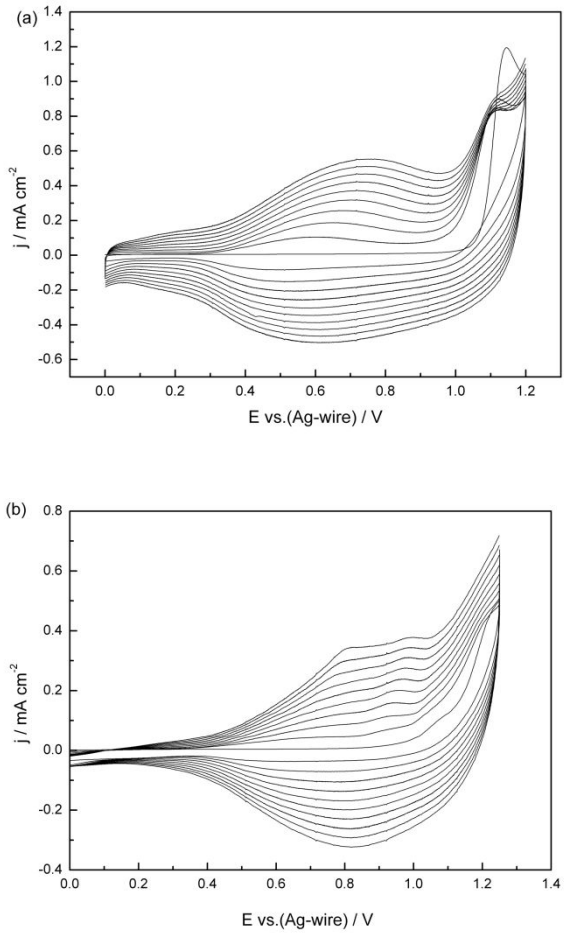

Fig. 1 Cyclic voltammogram curves of MOTTP (a) and BOTTP (b) in ACN/DCM (1:1) containing 0.2 M $TBAPF_6$ solutions at a scan rate of 100 mV s^{-1}

Stability and robustness of the polymer films are quite important parameters to be amenable for use in numerous practical applications. The stability of polymer film without purging the electrolyte solution with an inert gas was investigated in monomer free electrolyte solution by applying potential pulses. The polymer films were prepared on Pt wires by sweeping the potentials five cycles at 100 mVs^{-1} in acetonitrile (ACN)/dichloromethane (DCM) (1:1, by volume) solvent mixture containing 0.2 M $TBAPF_6$ and 0.005 M monomers and its cyclic voltamogram was recorded with cycled for 1000 times at 200 mVs^{-1} in monomer free electrolyte solution. The total charge involved during the electrochemical process was calculated for each voltammogram cycle. The Fig.3 showed the change of CV curves for PMOTTP and PBOTTP films between the 1st and 1000th cycles. As depicted in Fig. 3a, the loss of the total charge of PMOTTP was approximately 10% between initial and 1000th cycles. For PBOTTP, the loss of the total charge was approximately 11% between initial and 1000th cycle (see Fig.3b). The stability test was carried out without the exclusion of air in order to test the environmental stability of the polymers, since the presence of air has been supposed to cause a detrimental effect on the stability of materials.[12] We suspect that the observed loss is most probably due to the degradation reactions catalyzed by the presence of oxygen and the trace of water in the environment. On the other hand, the electropolymerization procedure in the environmental conditions may lead to the formation of oligomers, which impedes good film-forming properties and the adhesion to the substrate.

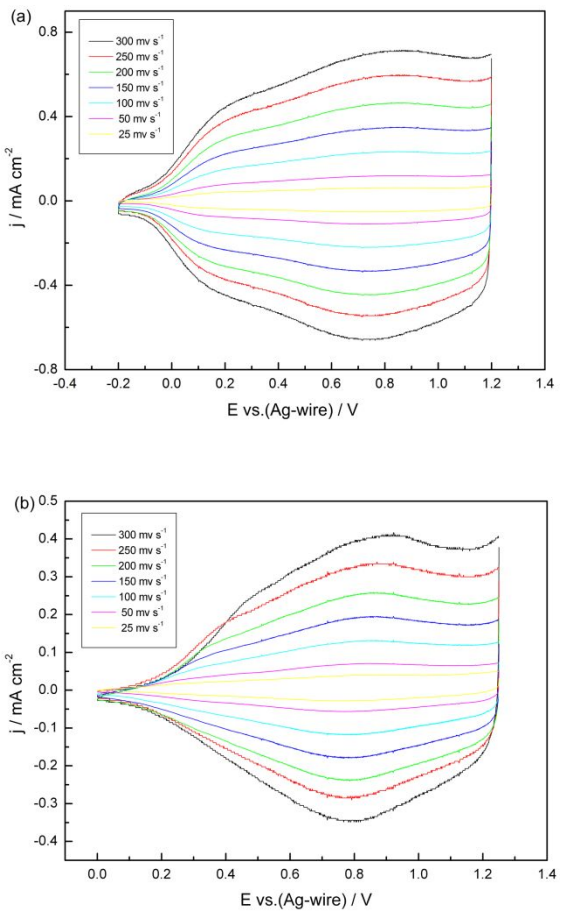

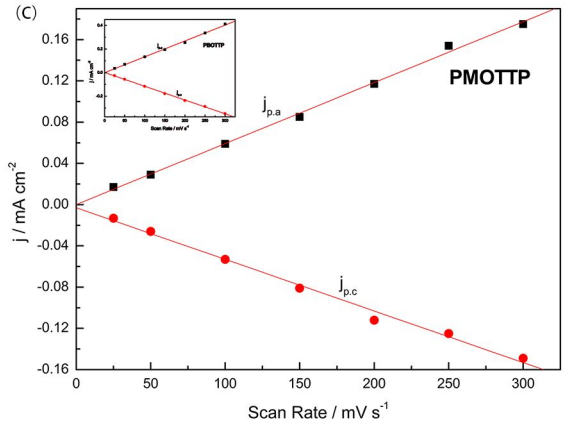

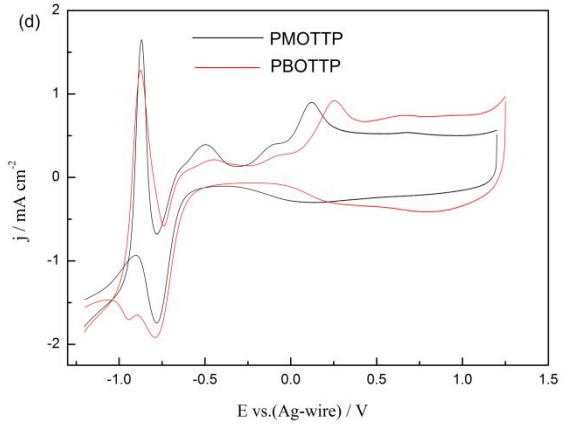

Fig. 2 CV curves of the PMOTTP (a) and PBOTTP (b) film at different scan rates between 25 and 300 mVs^{-1} in the monomer-free 0.2 M $TBAPF_6$ /ACN/DCM solution, respectively. (c) Scan rate dependence of the anodic and cathodic peak current densities graph of the p-doping/dedoping process. $j_{p.a}$ and $j_{p.c}$ the anodic and cathodic peak current densities, respectively. (d) The CV of PMOTTP and PBOTTP at scan rate 100mVs^{-1} in n-doping and p-doping process.

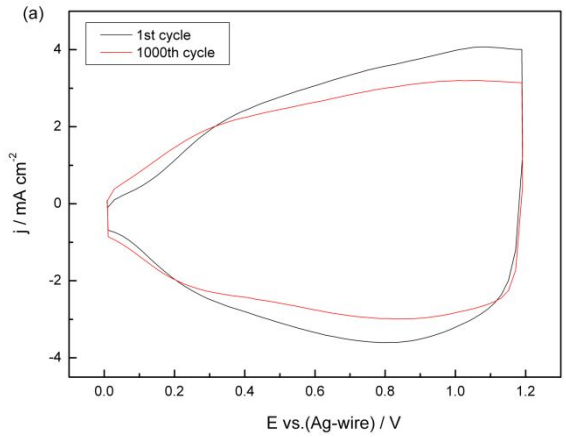

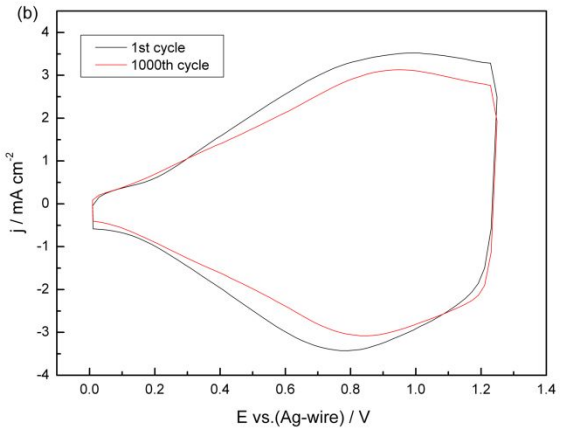

Fig. 3 Electrochemical stability of PMOTTP (a) and PBOTTP (b) in the monomer-free ACN/DCM (1:1) containing 0.2 M $TBAPF_6$ solutions after 1000 switching by CV method.

Morphology and thickness

The surface morphologies of polymer films were analyzed by SEM. The films were prepared by constant potential in the ACN/DCM (1:1, by volume) solution containing 0.2 M $TBAPF_6$ and 0.005 M relevant monomer on ITO electrode with the same polymerization charge of 3.0×10^{-2}C and dedoped before characterization. SEM images of these polymer films are shown in Fig.4a. As for PMOTTP film, it exhibits a compact morphology with the stack of granules. The diameters of granules range from 4 to 24 μm. While the PBOTTP film exhibits an irregular porous structure like coral grown with small granules. And the approximate diameters of granules are in the range of 2-12 μm. These morphologies can facilitate the movement of doping anions into and out of the polymer film during doping and dedoping process, in good agreement with the good redox activity of the films[37].

The thickness and roughness of polymer films were investigated by step profiler. The thickness images are shown in Fig.4b. As seen from Fig.4b, the thickness of PMOTTP and PBOTTP was 830 nm, 1002 nm respectively. The images of step profiler measurements reveal that the polymer films have extremely rough surface with detective pits, which is in good agreement with morphologies of SEM images. Fig.4b also revealed that PMOTTP had a lower average roughness value as compared to PBOTTP due to the compact morphology of PMOTTP.

Optical properties of the monomers and films

The UV-vis absorption spectra of monomers dissolved in CH_2Cl_2 and the corresponding dedoped polymer films which were deposited on ITO electrode were examined. And the absorption spectra of these novel monomers and films at neutral state were shown in Fig.5. As the Fig.5 presented, all two monomers exhibited two characteristic absorption bands as the typical feature of donor-acceptor conjugated compounds, which were assigned to the π-π* transition as well as intramolecular

charge transfer, respectively. Two obvious absorption peaks were observed at 308 and 482 nm for MOTTP, 309 and 487 nm for BOTTP. Meanwhile, the optical band gaps (E_g) of the monomers were calculated precisely from its low energy absorption edges (λ_{onset}) (E_g= 1241/λ_{onset}). The E_g of MOTTP and BOTTP based λonset (λ_{onset}=563 nm for MOTTP, 561 nm for BOTTP) were calculated as 2.20 eV, 2.21, eV respectively. Compared with MOTTP, BOTTP had a little blue shift of the low energy absorption band and a bit higher band gap due to the fact that the introduction of a longer butyl for replacement of methyl causes bigger steric hindrance, resulting in less order and less conjugation effect.

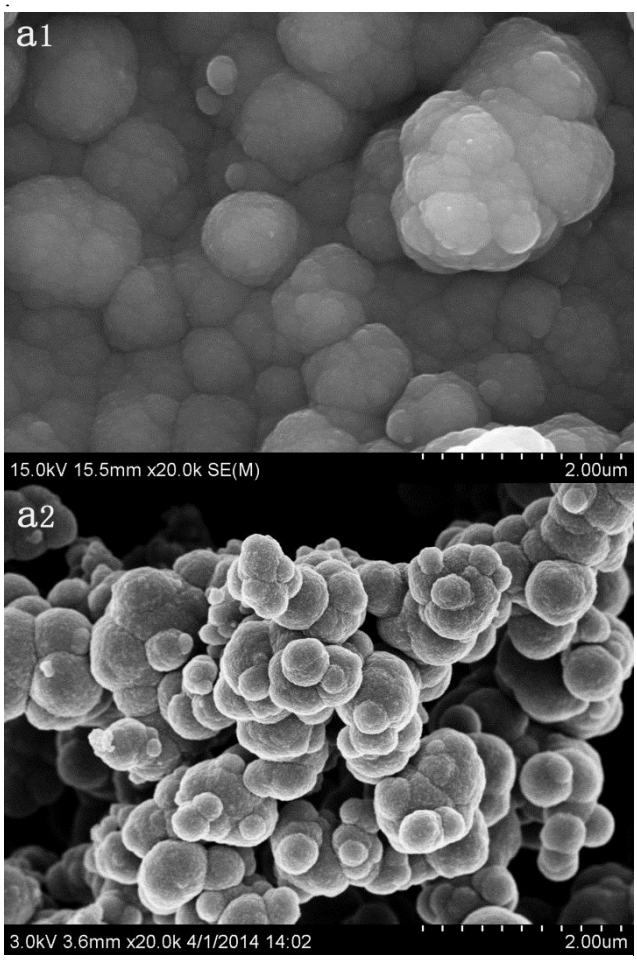

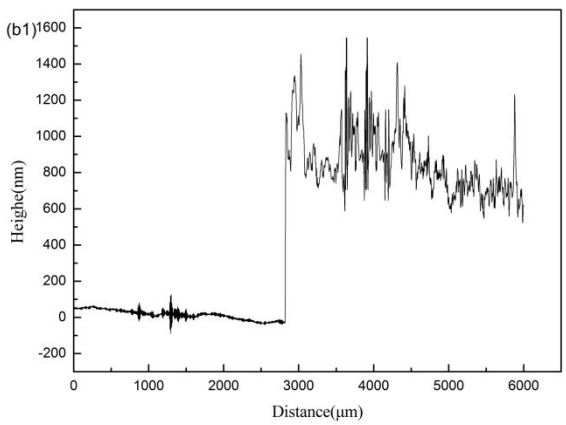

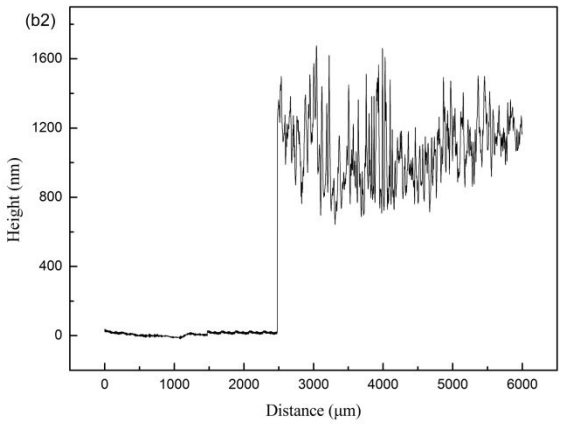

Fig. 4 SEM images of (a1) PMOTTP, (a2) PBOTTP and step profiler images of (b1) PMOTTP, (b2) PBOTTP deposited potentiostatically onto ITO electrode.

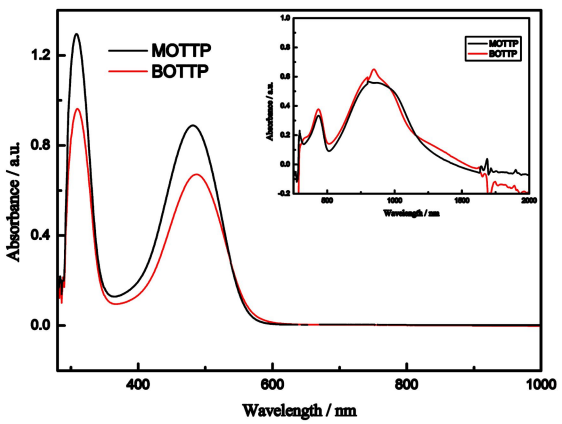

Fig. 5 UV-vis absorption spectra of MOTTP and BOTTP in DCM. inset: absorption spectra of the corresponding polymers deposited on ITO at the neutral state.

The UV-vis absorption spectra of the neutral state films were shown in the inset of Fig.5. The location of the absorption maximal and intensity of the peak on the main π-π* peak give some insight into a polymer color. As seen from inset of Fig.5, both polymers presented two well-separated maximal absorption peaks in visible region which were assigned to the strong π-π* transition and intramolecular charge transfer at neutral state, with the absorption peaks located at 435 nm and 850 nm for PMOTTP whereas for PBOTTP that located at 432 nm and 848 nm, which are essential values for a neutral green state. A minimum absorption is observed at around 514 nm for PMOTTP, and the differences in transmittance of the peaks at 435 and 850 nm are excellent to produce a highly saturated green color. The PBOTTP exhibited similarly

Table 1. The onset oxidation potential (E_{onset}), maximum absorption wavelength (λ_{max}), absorption onsets wavelength (λ_{onset}), HOMO and LUMO energy levels and optical band gap (E_g)

Compounds	E_{onset} (v)	λ_{max} (nm)	vs.(Ag-wire) λ_{onset} (nm)	E_g[a] (ev)	E_g[d] (ev)	HOMO[b] (ev)	LUMO[c] (ev)
MOTTP	1.06	308,482	563	2.20	1.956	-5.48	-3.28
BOTTP	1.07	309,487	561	2.21	2.032	-5.49	-3.28
PMOTTP	0.039	435,850	1300	0.95	-	-4.459	-3.509
PBOTTP	0.035	432,848	1140	1.088	-	-4.455	-3.367
PBDT[e]	-	428,755	1043	1.191	-	-	-

[a] calculated from the low energy absorption edges(λ_{onset}), Eg=1241/λ_{onset}
[b] HOMO = –e(E_{onset} + 4.4) (E_{onset} vs. SCE).
[c] calculated by the subtraction of the optical band gap from the HOMO level.
[d] E_g is calculated based on DFT.
[e] Data were taken from Ref[38].

spectroelectrochemistry behavior. The E_g of PMOTTP and PBOTTP based λ_{onset} (1300 nm for PMOTTP, 1140 nm for PBOTTP) were calculated as 0.95 eV, 1.088 eV, respectively (see Table 1). As shown in Table 1, PMOTTP has an apparent red shift of the low-energy absorption wavelengths and lower band gap than PBOTTP. It is suggested that the introduction of the butyl group on donor unit increased repulsive steric effect on neighboring repeat unit, which finally brought about the decrease of effective conjugation length in the homopolymer and a bit higher band-gap.[35] Moreover, the polymers experienced a red shift in the absorption maximal compared to the corresponding monomers, which was attributable to the inter chain interaction caused by π-stacking of the polymers. In addition, the parameters of 4,7-bis (2,3-dihydrothieno[3,4-b][1,4]dioxin-7-yl)benzo[c][1,2,5]thiadiazole (PBDT)[38] were also listed in Table 1 in order to compare with the newly prepared polymers. By contrast, the optical band gaps of PMOTTP and PBOTTP were somewhat lower than that of PBDT which demonstrated that PMOTTP and PBOTTP were more outstanding D-A type conducting polymers than PBDT.[38]

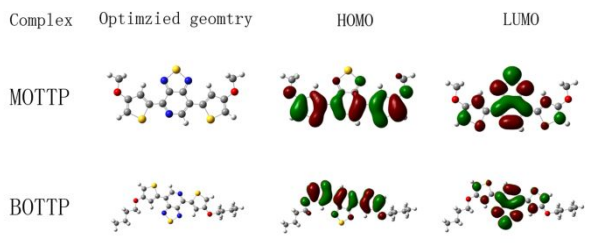

Fig.6 The ground-state electron density distribution of the highest occupied molecular orbital (HOMO) and lowest unoccupied molecular orbital (LUMO)

To obtain precise electrical band gap of monomers, DFT calculations were carried out on the density functional theory (DFT) level employing the Gaussian 05 programs. The ground-state electron density distribution of the highest occupied molecular orbital (HOMO) and lowest unoccupied molecular orbital (LUMO) are illustrated in Fig.6. The values of HOMO and LUMO are -5.627, -3.666 for MOTTP and -5.586, -3.554 for BOTTP. The band gap is calculated as 1.956, 2.032 for MOTTP and BOTTP respectively. These values were found lower than the values from experimentally data. This is mainly due to various effects such as solvent effects and to variation in solid state to the gaseous states. By contrast, the band gap of MOTTP based DFT calculation is bit lower than that of BOTTP, which is exactly consistent with the band gap based optical experiment.

In view of device and high-performance display applications, the optical properties of the polymers should be manifested by using the changes in optical absorption spectra under various voltage pulses. Potentiostatically deposition was performed in ACN/DCM (1:1, by volume) solution containing 0.2 M $TBAPF_6$ as a supporting electrolyte and 0.005 M monomers. The PMOTTP and PBOTTP films were electrodeposited onto ITO with the same polymerization charge of 2.0×10^{-2} C at 1.20 V, 1.25 V, respectively. After polymerization, electrochemical dedoping was carried out at 0 V in monomer free ACN/DCM (1:1, by volume) containing 0.2 M $TBAPF_6$ solution, then in situ electronic absorption spectra of polymer films were investigated upon stepwise oxidation. Fig. 7 reveals the spectroelectrochemistry and corresponding colors of PMOTTP and PBOTTP films. As seen from Fig.7, all polymers exhibited

two transitions due to their donor-acceptor nature at the neutral state. The two transitions in D-A type polymers were attributed to the transitions from the thiophene based valence band to its antibonding counterpart (high-energy transition) and to the substituent-localized conduction band (low energy transition). Hence, interactions between donor and acceptor units (their match) determined the energy and intensity of these transitions.[39] The intensities of low energy transitions for polymers are apparent higher than that of the corresponding high-energy transitions, as observed from the absorption peak in the visible region.

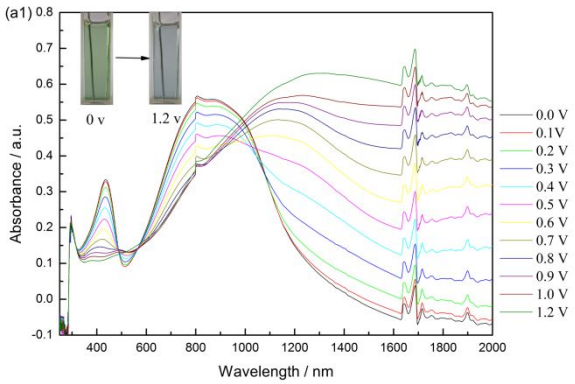

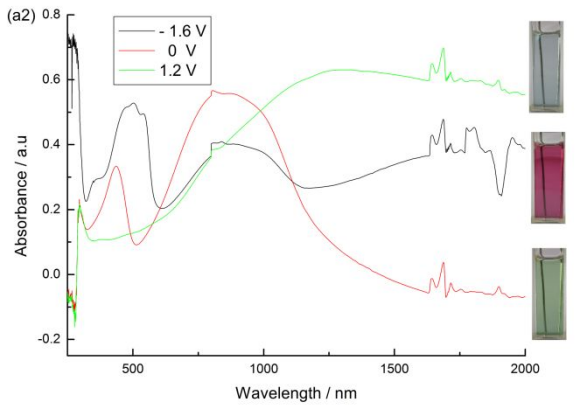

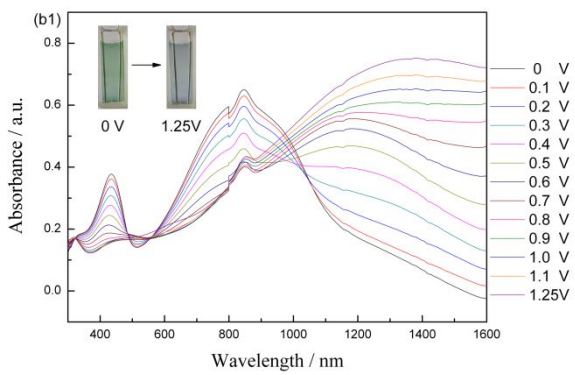

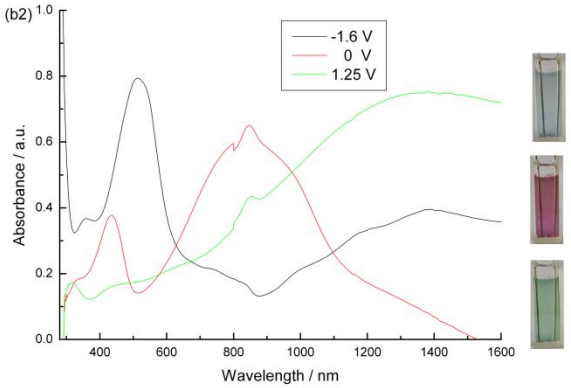

Fig. 7 (a1) p-doping: Spectroelectrochemistry of PMOTTP films on ITO electrode as applied potentials between 0 V and 1.2 V in the monomer-free 0.2 M $TBAPF_6$ /ACN/DCM solution. (a2) n-doping: Spectroelectrochemistry of PMOTTP films at -1.6, 0 and 1.2 V. (b1) p-doping: Spectroelectrochemistry of PBOTTP filmson ITO electrode as applied potentials between 0 V and 1.25 V in the monomer-free 0.2 M $TBAPF_6$ /ACN/DCM solution. (b2) n-doping: Spectroelectrochemistry of PBOTTP films at -1.6, 0 and 1.25 V.

To further elucidate the optoelectronic properties of these thin polymer films, in situ spectroelectrochemical measurements are performed wherein the obsorption spectra are measured as increasingly higher oxidizing potentials are applied across the polymer film. As shown in Fig.7 a1, upon oxidation of the polymer PMOTTP, the intensity of the absorption of the two π-π* transition bands (centered at 435 and 850 nm, respectively) started to decrease simultaneously with a concomitant increase in the near-IR region (beyond 1400 nm), indicating the formation of polaron[40] and bipolaron.[41] At the fully oxidized state of the polymer PMOTTP (1.2 V), the newly formed lower energy electronic transitions lie sufficiently outside the visible region with little tailing from the NIR, which make the polymer present highly transmissive blue color in the oxidized states. In this case, PMOTTP can switch between the neutral green color to the high transmissive blue color in the oxidized state. As indicated in Fig.7 b1, PBOTTP film experienced a similar change trend with that of PMOTTP as the potentials stepped from 0 V (neutral state) to 1.25 V (oxidized state). UV-vis spectra for PMOTTP and PBOTTP (Fig.7) display well-defined isosbestic points at approx. 564 nm and 558 nm respectively, indicating that PMOTTP and PBOTTP polymers were being interconverted between two distinct forms on both occasions: the neutral form and radical cation.[39]

Conducting polymers with stable negatively doped states receive a tremendous interest, since a more complicated device structure such as LEDs[3] and ambipolar field effect transistors can be attained with these materials. In addition to reduction waves in CV, evidence for charge carrier formation upon reduction should also be studied by spectroelectrochemistry. Absorption spectrums of polymers at the reduction potential of -1.6 V were investigated to characterize the optical changes that occurred during the n-doped process and prove the introduction of charge carriers to the conjugated systems at n-doped state. As shown in Fig.7, upon the switch from the neutral to the reduced state, several similar changes have been seen for the UV-vis-NIR spectra of the two polymers, including the

Table 2. The values of L, a ,b of polymers in neutral , oxidized and reduced states.

Polymers	E,vs.(Ag wire)(V)	L	a	b	Colors
PMOTTP	0	61	-9	11	Saturation green
	1.2	60	-5	-4	Saturation green
	-1.6	42	43	-1	Red
PBOTTP	0	63	-17	13	Saturation green
	1.25	60	-4	-1	Transmission blue
	-1.6	43	25	2	Red

Table 3. The optical contrasts (ΔT%), response times and coloration efficiencies (CE) of the PMOTTP, PBOTTP and PBDT at corresponding wavelengths.

Compounds	λ nm	Optical contrast (ΔT %)	Response time (s)	Coloration efficiency (CE cm^2C^{-1})
PMOTTP	430	24	0.44	76.9
	1550	70	0.43	249
PBOTTP	435	32	0.51	99
	1500	61	0.55	259
PBDT[a]	428	37	< 1	-
	755	23	0.40	-
	1500	72	≈ 1	-

[a] Data were taken from Ref[39].

moderate absorption increase in the NIR region, the weakening even vanishment of the absorption band at around 850 nm, the red-shift of the π-π* transition band, and the appearance of the apparent and well-defined absorption peaks at around 500 nm in the visible region. The maximum absorption peaks were centered at 508 nm and 512 nm for PMOTTP and for PBOTTP, respectively, which give rise to a saturated red color in the reduced states of the polymers. Hence, with strong absorption changes in the NIR region and the CV waves observed at negative potentials, it is clear that both PMOTTP and PBOTTP are revealing true n-type doping processes.[37] It is interesting that these polymers are unique in the literature with its highly saturated green color in the neutral state and high transmissive blue in the oxidized state and saturated red in the reduced state up to date. To further establish the colors of polymers, the colorimetric properties were characterized by CIE1976 color space (L*a*b*). The values of the relative luminance (L), hue (a) and saturation (b) were measured at the neutral, oxidized and reduced states of polymers and summarized in Table 2.

Switching properties

The stabilities, optical contrasts, and response times upon electrochromic switching of the polymer films between their neutral and oxidized states have been monitored both in the visible and NIR regions. The studies were performed with a switching interval of 4 s at their dominant wavelengths by multi-potential steps repeatedly between their fully neutral and oxidized states in a monomer free ACN/DCM (1:1,by volume) solution containing 0.2 M $TBAPF_6$ as a supporting electrolyte. The optical contrasts, response time as well as coloration efficiencies of PMOTTP, PBOTTP and PBDT based on electrochromic switching at different given wavelengths were shown in Table 3. PBDT was used to compared with the newly polymers. The optical contrast (ΔT%), one of the crucial factors in appraising an electrochromic material, is defined as a percent transmittance change at a specified wavelength between the redox states. Fig.8 reveals the electrochromic switching properties of PMOTTP between 0 and 1.2 V and PBOTTP between 0 and 1.25 V at two different wavelengths both in visible and NIR regions. The optical contrasts of PMOTTP (24% at 430 nm, 70% at 1550 nm) and PBOTTP (32% at 435 nm, 61% at 1500 nm) are satisfactory. Compared with the structural analogue polymer of PBDT, the newly prepared polymers have comparable optical contrasts in both the visible and the NIR region. The outstanding optical contrast in the NIR region is a very significant property for many NIR applications. After 1000 cycles switching, polymers kept working without significant loss in percent transmittance contrast value. It indicated that polymers has quite high optical stability, retaining 96% at 430 nm and 97% at 1550 nm for PMOTTP and 94% at 435 nm and 95% at 1500 nm for PBOTTP after 1000 cycles switch.

Response time, another most important characteristic of electrochromic materials, is the necessary time for 95% of the full optical switch (after which the naked eye could not sense the color change).[42] PMOTTP has excellent switching times of 0.439 s at 430 nm and 0.438 s at 1550 nm from neutral to oxide, respectively. PBOTTP has comparable switching times of 0.510 s at 435 nm and 0.550 s at 1500 nm. By contrast, it can be easily found that PMOTTP film showed a tiny bit faster switch time than that of PBOTTP. faster switching response could be ascribed to the faster dopant ion diffusion during the redox process. Compared with PBDT,[38] the switch time of

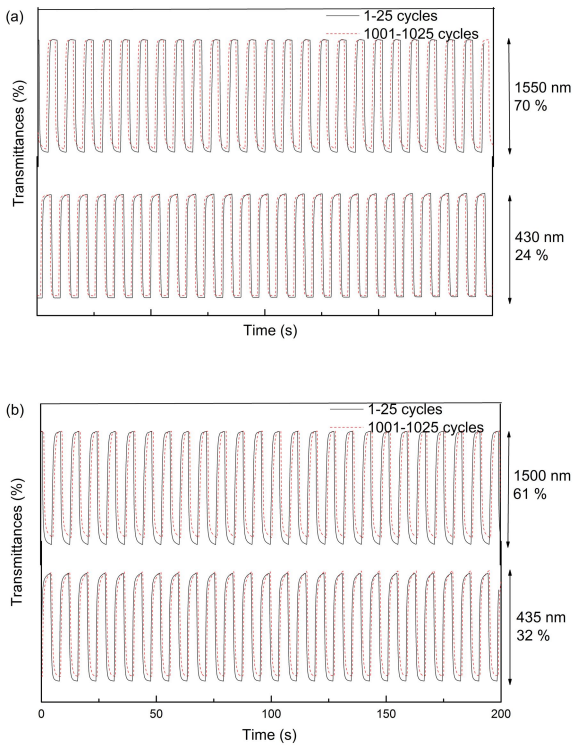

Fig. 8 (a) Electrochromic switching, percent transmittance change monitored at 430 and 1550 nm for PMOTTP between 0 and 1.2 V. (b) Electrochromic switching, percent transmittance change monitored at 435 and 1500 nm for PBOTTP between 0 V and 1.25 V.

switch time of the newly polymers is faster than that of PBDT in NIR region and is comparable in the visible region.

The coloration efficiency (CE) is also an important characteristic for electrochromic materials, which is defined as the relation between the injected/ejected charge as a function of electrode area (ΔQ) and the change in optical density (ΔOD) at a specific dominant wavelength (λ_{max}) as illustrated by the following equation[40].

$$\Delta OD = \log\left(\frac{T_b}{T_c}\right) \qquad \eta = \frac{\Delta OD}{\Delta Q}$$

Where the T_b is the transmission in the bleached state and T_c is the transmission in the colored state. T_c and T_b values are measured at a nominated wavelength (typically the wavelength producing the maximum optical density change, $\Delta OD_{\lambda max} = \log(T_b/T_c)_{\lambda max}$). ΔQ is the charge density, the charge ingress/egress divided by the geometric electrode area of the polymer. CE is expressed in units of $cm^2\ C^{-1}$. The coloration efficiency of the PMOTTP was found to be 76.9 cm^2C^{-1} for 430 nm and 249 cm^2C^{-1} for 1550 nm during the p-doping process; whereas 99 cm^2C^{-1} for 435 nm and 259 cm^2C^{-1} for 1500 nm for PBOTTP.

Conclusions

Novel D-A type monomers based on [1,2,5]thiadiazolo[3,4-c]pyridine (PT) as the acceptor unit and alkoxy thiophene as the donor as well as corresponding polymers have been successfully synthesized by electropolymeration to understand the effects of different electron donating groups on electrochemical and optoelectronic properties. Electrochemical and spectroelectrochemical characterization demonstrate that methoxythiophene and butoxythiophen were strong electron-donor and the properties of PBOTTP were inferior to that of PMOTTP due to the steric hindrance of butyl. The optical band gaps of PMOTTP and PBOTTP were 0.950, 1.088 eV, respectively. The corresponding polymer films revealed a saturated green color in the neutral state, a saturated red in the reduced state and a highly transmissive blue in the oxidized state which realized RGB in one polymer. At the same time, the outstanding optical contrasts in the NIR region (appro. 60%), very fast switching times (about 0.5 s) and high enviromental stabilities make these polymers paramount choices for the green component of polymer electrochromic display applications. Moreover, the existence of the n-type doping process was proved by both electrochemical and spectral analysis for films. Efforts to combine new streams of thought for further flowering of this already fertile field are still in progress and the results will be reported in due course.

Acknowledgements

The work was financially supported by the National Natural Science Foundation of China (51473074,31400044), the General and Special Program of the postdoctoral science foundation China (2013M530397, 2014T70861).

Notes and references

[a] College of Chemical Engineering, China University of Petroleum (East China), QingDao, 266580, P. R. China

[b] Shandong Key laboratory of Chemical Energy Storage and Novel Cell Technology, Liaocheng University, Liaocheng, 252059, P. R. China

Corresponding authors. E-mail addresses: j.s.zhao@163.com (J. Zhao) ; jmdou@lcu.edu.cn (jianmin dou)

† Electronic Supplementary Information (ESI) available: ^{1}HNMR and ^{13}CNMR spectra of the intermediates and target compounds.

1 C. K. Chiang, C. R. Fincher, Y. W. Park, A. J. Heeger, H. Shirakawa, E. J. Louis, S. C. Gau, A. G. MacDiarmid, *Phys. Rev. Lett.*, 1977, **39**, 1098-1101.

2 C. J. Brabec, N. S. Sariciftci, J. C. Hummelen, *Adv. Funct. Mater.*, 2001, **11**, 15.

3 R. J. Mortimer, *Chem. Soc. Rev.*, 1997, **26**, 147–156.

4 N. Stutzmann, R. H. Friend, H. Sirringhaus, *Science*, 2003, **299**, 1881.

5 D. T. McQuade, A. E. Pullen, T. M. Swager, *Chem. Rev.*, 2000, **100**, 2537.

6 P. K. H. Ho, D. S. Thomas, R. H. Friend, N. Tessler, *Science*, 1999, **285**, 233.

7 I. Schwendeman, R. Hickman, G. Sonmez, P. Schottland, K. Zong, D. M. Welsh, J. R. Reynolds, *Chem. Mater.*, 2002, **14**, 3118.

8 G. Sonmez, H. Meng, Q. Zhang, F. Wudl, *Adv. Funct. Mater.*, 2003, **13**, 726.

9 A. A. Argun, P. H. Aubert, B. C. Thompson, I. Schwendeman, C. L. Gaupp, J. Hwang, N. J. Pinto, D. B. Tanner, A. G. MacDiarmid, J. R. Reynolds, *Chem. Mater.*, 2004, **23**, 4401–4412.

10 M. M. Verghese, M. K. Ram, H. Vardhan, B. D. Malhotra, S. M. Ashraf, *Polymer*, 1997, **38**, 1625–1629.

11 D. N. Buckley, L. D. Burke, *J. Chem. Soc. Faraday Trans.,* 1975, **1**, 1447.
12 L. Groenendaal, G. Zotti, P.-H. Aubert, S. M. Waybright, J. R. Reynolds, *Adv. Mater.,* 2003, **15**, 855.
13 S. A. Sapp, G. A. Sotzing, J. R. Reynolds, *Chem. Mater.,* 1998, **10**, 2101.
14 A. Kumar, D. M. Welsh, M. C. Morvant, K. A. Abboud, J. R. Reynolds, *Chem. Mater.,* 1998, **10**, 896.
15 G. Sonmez, H. B. Sonmez, K. F. Shen, R. W. Jost, Y. Rubin, F. Wudl, *Macromolecules*, 2005, **38**, 669.
16 P. M. Beaujuge, J. R. Reynolds, *Chem. Rev.*, 2010,**110**, 268–320.
17 Sonmez, *Chem. Commun.,* 2005, 5251–5259.
18 G. Sonmez, C. K. F. Shen, Y. Rubin, F. Wudl, Angew. *Chem. Int. Ed.,* 2004, **116**, 1498.
19 A. Ennisi, F. Simone, G. Barletta, G. Di Marco, L. Lanza, *Electrochim. Acta,* 1999, **44**, 3237.
20 J. Mao, J. Yang, J. Teuscher, T. Moehl, C. Yi, R. Humphry-Baker, P. Comte, C. Grätzel, J. Hua, S. M. Zakeeruddin, H. Tian and M. Grätzel, *J. Phys. Chem. C,* 2014, 140421130119006.
21 P. M. Beaujuge, S. Ellinger and J. R. Reynolds, *Adv. Mater.,* 2008, **20**, 2772-2776
22 A. Durmus, G. E. Gunbas, P. Camurlu, L. Toppare, *Chem. Commun.*, 2007, 3246.
23 A. Durmus, G. E. Gunbas, L. Toppare, *Chem. Mater.*, 2007, **19**, 6247.
24 G. E. Gunbas, A. Durmus, L. Toppare, *Adv. Funct. Mater.,* 2008, **18**, 2026.
25 G. E. Gunbas, A. Durmus, L. Toppare, *Adv. Mater.*, 2008, **20**, 691–695.
26 F. Ozyurt, E. G. Gunbas, A. Durmus, L. Toppare, *Org. Electron.*, 2008, **9**, 296–302.
27 Y. A. Udum, A. Durmus, G. E. Gunbas, L. Toppare, *Org. Electron.*, 2008, **9**, 501–506
28 D. Baran, G. Oktem, S. Celebi and L. Toppare, *Macromol. Chem. Phys.,* 2011, **212**, 799-805.
29 N. Blouin, A. Michaud, D. Gendron, S. Wakim, E. Blair, R. Neagu-Plesu, M. Belletête, G.Durocher, Y. Tao, M.Leclerc, *J. Am. Chem. Soc.*, 2008, **130**, 732−742.
30 Y. Sun, G. C. Welch, W. L. Leong, C. J. Takacs, G. C. Bazan, A. J. Heeger, *Nat. Mater.*, 2012, **11**,44−48.
31 A. Balan, D. Baran, G. Gunbas, A. Durmus, F.Ozyurt, L. Toppare, *Chem. Commun*., 2009, **44**, 6768.
32 W. Ying, X. Zhang, X. Li, W. Wu, F. Guo, J. Li, H. Ågren and J. Hua, *Tetrahedron*, 2014, **70**, 3901-3908.
33 X. X. Sun, Y. Z. Lou, Q. Q. Chen, L. Li, X. X. Zhuang and Y. C. Li, *Advanced Materials Research*, 2011, **335-336**, 90-95.
34 Q. Hou, Q. Zhou, Y. Zhang, W. Yang, R. Yang, Y. Cao, *Macro.*, 2004, **37**, 6299-6305
35 A. Kraft, A. C. Grimsdale, A. B. Holmes, Angew. *Chem., Int. Ed.,* 1998, **37**, 403–428.
36 D. M. de Leeuw, M. M. J. Simenon, A. R. Brown, R. E. F. Einerhand,; *Synth. Met.,* 1997, **87**, 1, 53.
37 M. İ. Özkut, S. Atak, A. M. Önal and A. Cihaner, *J. Mater. Chem.*, 2011, **21**, 5268.
38 D. Baran, G. Oktem, S. Celebi and L. Toppare, *Macromol. Chem. Phys.*, 2011, **212**, 799-805.
39 H. Akpınar, A. Balan, D. Baran, E. K. Ünver, L. Toppare, *Polymer,* 2010, **51**, 6123-6131.
40 J. J. Aperloo, R. A. J. Janssen, *Synth. Met.,* 1999, **101**, 417.
41 B. Sankaran, J. R. Reynolds, *Macromolecules,* 1997, **30**, 2582.
42 A. Cihaner, F. Algı, *Electrochim. Acta.,* 2008, **54**, 786-792.

Graphical Abstract

Two Novel Ambipolar Donor-Acceptor Type Electrochromic Polymers with the Realization of RGB (Red-Green-Blue) Display in one Polymer

Hui Zhao[1], Daidi Tang[1,2], Jinsheng Zhao[2,]*and Min Wang[2]

Two novel D-A type polymers were synthesized and characterized, which realized the valuable full color display in only one polymer.